JOURNAL OF MATERIALS SCIENCE 20 (1985) 689–699

Effects of manganese and ageing on martensitic transformation of Cu–Al–Mn alloys

KENICHI MATSUSHITA, TAKASHI OKAMOTO, TAIRA OKAMOTO
The Institute of Scientific and Industrial Research, Osaka University, Ibaraki, Osaka 567, Japan

Manganese lowered the M_s temperature of Cu–Al–Mn alloys by about 30 K per 1 wt % Mn and prevented precipitation of stable phases from the supercooled β phase. Precipitation of stable phases interfered with growth of martensite plates and made transformation hysteresis larger.

1. Introduction

Cu–Al base alloys water-quenched from the β phase field causes thermoelastic martensitic transformation below the M_s temperature. Since shape memory effect and high damping capacity of the alloys, in general, have been associated with the transformation, this transformation has interested many investigators [1–4]. M_s temperatures of the alloys are sensitive to the cooling rate during quenching, because the cooling rate relates to the completeness of ordering of β [5], the decomposition of β and β_1 to α and γ_2, and vacancy concentration [6]. It is known that water-quenching of a Cu–Al binary alloy could not completely prevent β and its ordered phase, β_1, from decomposition to stable phases [7]. Therefore, an element, such as nickel and zinc, was added into Cu–Al binary alloys as a third element to stabilize β and β_1.

From a preliminary experiment, the present authors knew that manganese also acted as a stabilizing element for β and β_1 and had a large effect in improving the ductility of Cu–Al alloys. Effects of manganese and ageing on martensitic transformation in Cu–Al and Cu–Al–Mn alloys were investigated with Cu–14 wt % Al binary alloys and Cu–13.5 wt % Al–Mn alloys containing 1.0 to 6.3 wt % Mn.

2. Experimental procedure

Four kinds of Cu–Al alloys and six kinds of Cu–Al–Mn alloys were made from electrolytic copper, pure aluminium of 4N purity, and Mn–11 wt % Cu alloy which was made from electrolytic manganese and electrolytic copper. Each mixture of these materials of about 800 g in total weight was melted in an alumina crucible under an argon atmosphere using a high frequency induction furnace and then was cast into an iron mould. The dimensions of the ingots were about 18 cm long, and 2.5 cm square section. Each ingot was sealed in an evacuated fused-silica tube and then was homogenized at 1173 K in the β phase field for 7 days. The chemical composition of the ingots is tabulated in Table I.

Specimens for electrical resistance measurements were prepared from the middle part of each homogenized ingot, the former being wire of 3.0 cm long and a square cross-section of 0.15 cm × 0.15 cm. All the specimens were held in an argon atmosphere at 1173 K for 2 h to produce a β phase and then were quenched into a 5 wt % KOH aqueous solution containing ice. In this heat treatment, vaporization of manganese in the specimens was too little to influence the manganese concentration at the surface.

The hot junction of a chromel–alumel thermocouple was set at the centre of each specimen for electrical resistance measurements. A specimen was fixed on a glass plate in a furnace after two of four lead wires were spot-welded on to the two sides of the specimen and the other two at a distance of 0.1 cm from each side. This specimen was cooled and then heated cyclically at a

0022–2461/85 $03.00 + .12

TABLE I Chemical composition and the M_s temperature of alloys prepared in the present study

Alloy	Chemical Composition (wt %)				M_s (K)
	Al	Mn	Cu	Al/(Cu + Al)	
A	13.5	1.0	85.5	13.64	< 450
B	13.5	2.3	84.2	13.82	337
C	13.7	1.5	84.8	13.91	313
D	13.7	1.9	84.4	13.97	293
E	13.6	3.2	83.2	14.05	243
F	13.4	6.3	80.3	14.30	100
G	13.82	–	86.18	13.82	> 640
H	14.03	–	85.97	14.03	328
I	14.17	–	85.83	14.17	285
J	14.36	–	85.64	14.36	290

constant rate of 0.033 K sec^{-1} under a nitrogen atmosphere following a diagram given for each alloy. In Fig. 1, an example of diagram for alloy B is shown. During heating, cooling and ageing at given temperatures for 30 min, electrical resistance of specimens was measured against temperature or elapsed time. The electrical resistance changes linearly with temperature unless phase transformation and decomposition occur in the specimen. The occurrence of martensitic transformation in specimens during cooling increases the electrical resistance. Therefore, the M_s temperature of a specimen can be determined as the temperature at which the electrical resistance–temperature plot obtained during cooling of the specimen deviates from linearity. The M_f, A_s and A_f temperatures were also determined in a similar way.

Phases existing in aged specimens were identified by the X-ray powder diffraction method. In this method, Cu$K\alpha$ radiation was used through a nickel filter. For the experiment, a slice was cut off from a homogenized alloy ingot and it was reduced to chips by drilling. Subsequently, the chips were ground into powder of about 50 mesh screen size. The powder obtained was quenched from the β phase field and heat-treated cyclically under similar condition to specimens for electrical resistance measurements. Furthermore, some ageing temperatures were taken in addition to the ageing temperatures in the programme.

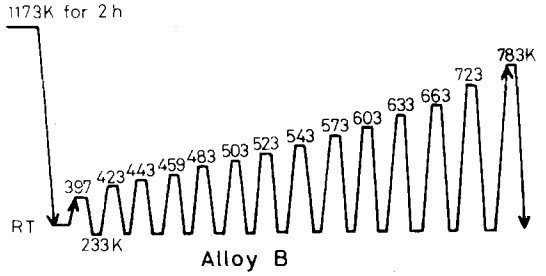

Figure 1 Heat treatment diagrams for alloys B.

3. Results

3.1. Effect of ageing on martensitic transformation temperatures

Electrical resistance–temperature curves for all the alloys except the alloys ageing at various temperatures are shown in Fig. 2. Since electrical resistance of martensite is higher than that of its master phase, the martensitic transformation always increases the electrical resistance and the reverse transformation decreases it. From the results given in Fig. 2, M_s, M_f, A_s and A_f temperatures of alloys B, D, E, H, I and J were determined as a function of ageing temperature, as shown in Fig. 3.

Alloy B had a M_s temperature above room temperature in the as-quenched state. With increasing ageing temperature, the M_s temperature of this alloy decreased to a minimum at 500 K and then increased in the temperature range between 500 and 600 K, as shown in Fig. 3a. It became a minimum at 633 K again. As for the M_f temperatures, this alloy had two minima at 500 and 600 K on the M_f temperatures–ageing temperature plot. The effect of ageing temperature on both M_s and M_f temperatures differed apparently. The difference between these temperatures, (martensitic transformation temperature range), was the largest on ageing at 600 K and was much wider on ageing at temperatures above 600 K rather than at temperatures below it (see Fig. 9).

Changes in electrical resistance accompanied by martensitic transformation, $\Delta R_T = (R_M - R_{\beta_1})/R_{T_0}$, in the same alloys as illustrated in Fig. 3 are plotted as a function of ageing temperature in Fig. 4. R_{T_0} is the electrical resistance at the temperature T_0, that is the mean temperature of M_s and M_f temperatures, and R_M and R_{β_1} are the electrical resistance of the phases after and before martensitic transformation at temperature T_0, respectively. These values can be determined by extrapolation of the electrical resistance–temperature plots below the M_f temperature and above the M_s temperature, respectively, as shown in Fig. 4. The values of ΔR_T for alloy B were small at ageing temperatures below 573 K and large above 600 K. It is noted that the largest value of ΔR_T was obtained on ageing at 723 K, though

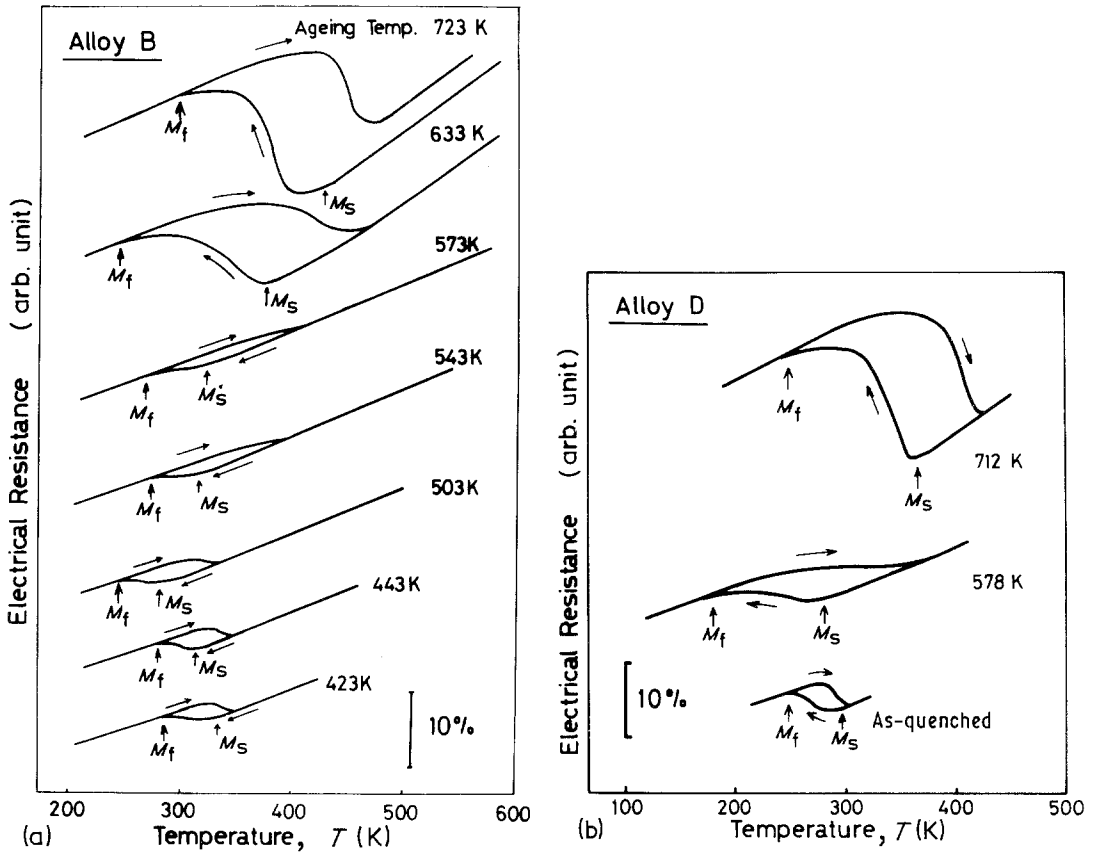

Figure 2 Electrical resistance against temperature curves of alloys B, D, E, H, I and J after ageing at the temperatures indicated in the figure for 30 min, are shown in (a), (b), (c), (d), (e) and (f), respectively.

the tendency of the β_1 phase to transform to martensite became less in quantity because of decomposition to stable phases as will be described below. When aged at 783 K, the alloy had no inflection point on the electrical resistance–temperature plot. This means that β_1 could not transform to thermoelastic martensite.

The M_s and M_f temperatures of alloy D, which were determined from electrical resistance–temperature curves shown in Fig. 2b, are plotted against ageing temperature in Fig. 3a. They decreased with a rise in the ageing temperature from 425 to 530 K and then increased with a further rise from 530 K. The martensitic transformation temperature range tends to increase on the whole without appreciable peaks and valleys with rising ageing temperature. On the other hand, the change of the value of ΔR_T with ageing temperature was like that for alloy B, that is, the value of ΔR_T increased considerably on ageing above 600 K, as shown in Fig. 4.

In the as-quenched specimen of alloy E, there was no martensite at room temperature because of the M_s temperature lower than room temperature. The M_s temperature was unvaried on ageing below 475 K. As seen from Fig. 3a, it was lowered with a rise in ageing temperature from 475 to 533 K and rose with a further rise in temperature from 650 to 900 K. The M_f temperature behaved against ageing temperature in a similar manner to the M_s temperature, though there was little difference in the ageing temperature range between 533 and 650 K. When comparing the M_s or M_f temperature against ageing temperature plot for alloy E with that for alloy B, the former had only one minimum, while the latter had two minima. The martensitic transformation temperature range of alloy E was the broadest on ageing at 568 K (see Fig. 9). With a rise in ageing temperature from 650 K, it became considerably larger again.

The value of ΔR_T accompanied by a martensitic transformation in alloy E was as large as ~ 22% in the as-quenched state, as shown in Fig. 4. This value was unchanged on ageing at temperatures

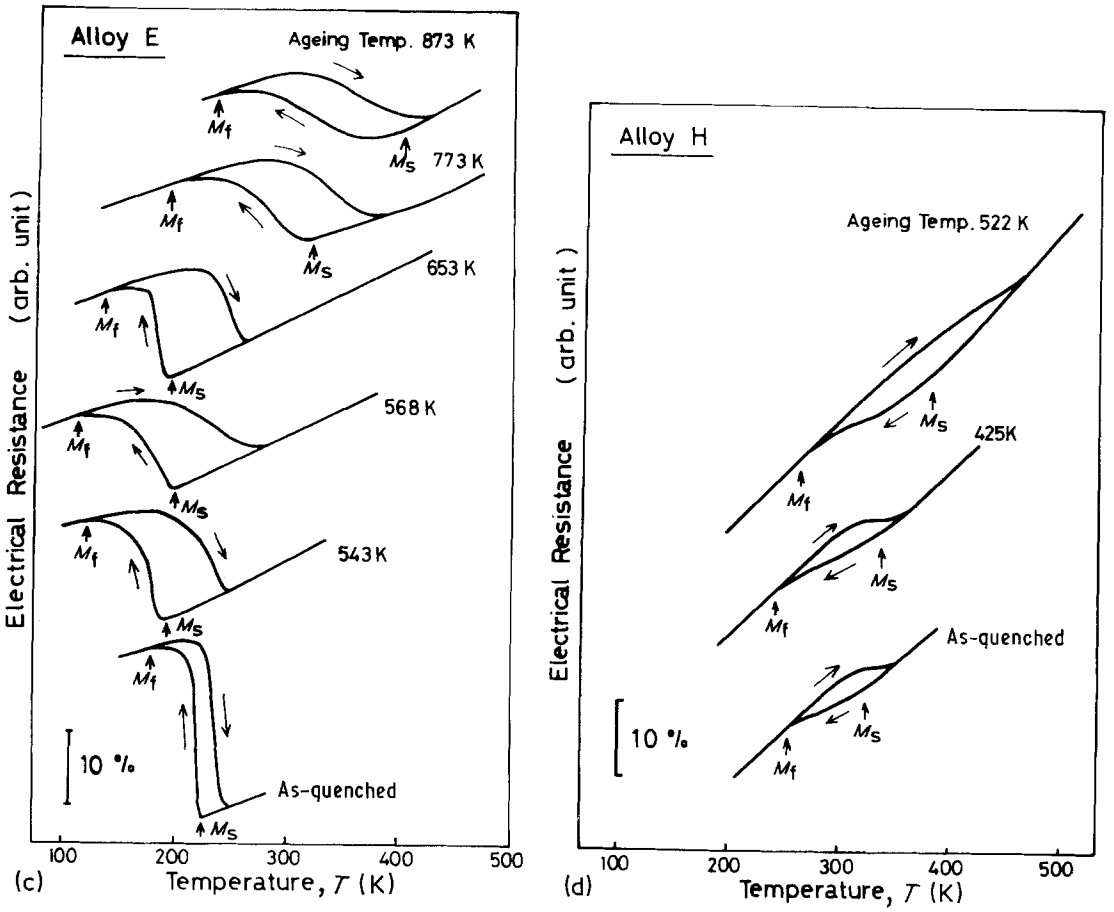

Figure 2 Continued.

below 507 K and was lowered to 14–17% at ageing temperatures above 541 K. Similarly to alloy B, two kinds of martensite also appeared, one was formed on ageing below 573 K and other above 600 K. The nature of the martensites was not examined in detail.

Fig. 2d shows electrical resistance–temperature plots for alloy H without manganese. The M_s and M_f temperatures of this alloy in the as-quenched state were ~330 and ~265 K, respectively. The effect of ageing temperature on these temperatures is illustrated in Fig. 3b. The M_s temperature became a minimum at 475 K and increased on ageing at a higher temperature above 500 K. The martensitic transformation temperature range increased with increasing ageing temperature (see Fig. 9). The value of ΔR_T accompanied by a martensitic transformation in alloy H increased gradually with increasing temperature, as known from Fig. 4, but it was lower than that of alloy D whose effective aluminium content, [%Al/(%Cu + %Al)] × 100, was a little higher than that of alloy H at all ageing temperatures. When aged over 600 K, alloy H hardly transformed to martensite.

Electrical resistance–temperature plots of alloy I without manganese are shown in Fig. 2e. The plot profile in the as-quenched state was similar to that of alloy H. The M_s and M_f temperatures of this alloy in the as-quenched state were about 285 and 262 K, respectively. The effect of ageing temperature on these temperatures is illustrated in Fig. 3b. The M_s temperature rose on ageing at a higher temperature above 500 K. The M_f temperature became a minimum at 502 K and rose on ageing at a higher temperature above 502 K. The martensitic transformation temperature range (M_s–M_f) increased with increasing ageing temperature but decreased at a higher ageing temperature above 575 K (see Fig. 9). The value of ΔR_T accompanied by a martensitic transformation in alloy I increased with an increase in ageing temperature from 424 to 502 K, as shown in Fig. 4. The A_s and A_f temperatures did not appear in the electrical resistance–temperature curve of

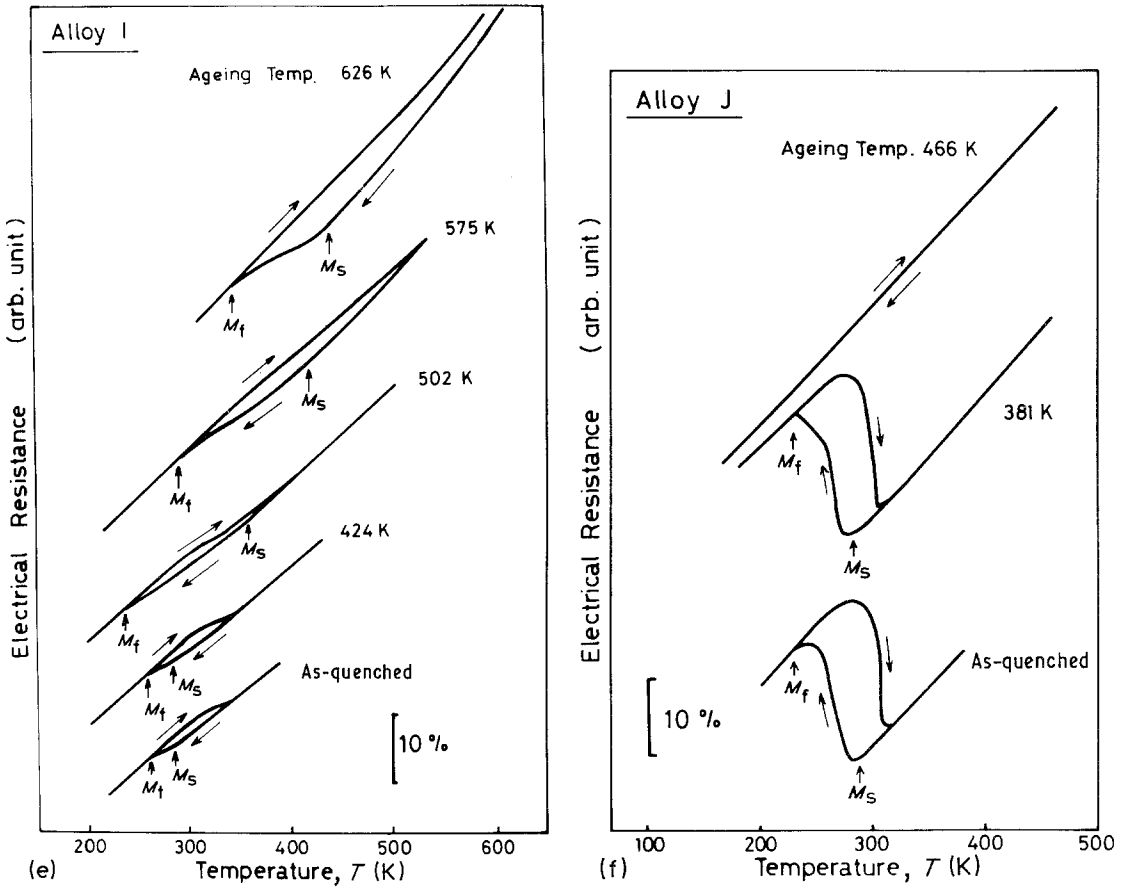

Figure 2 Continued.

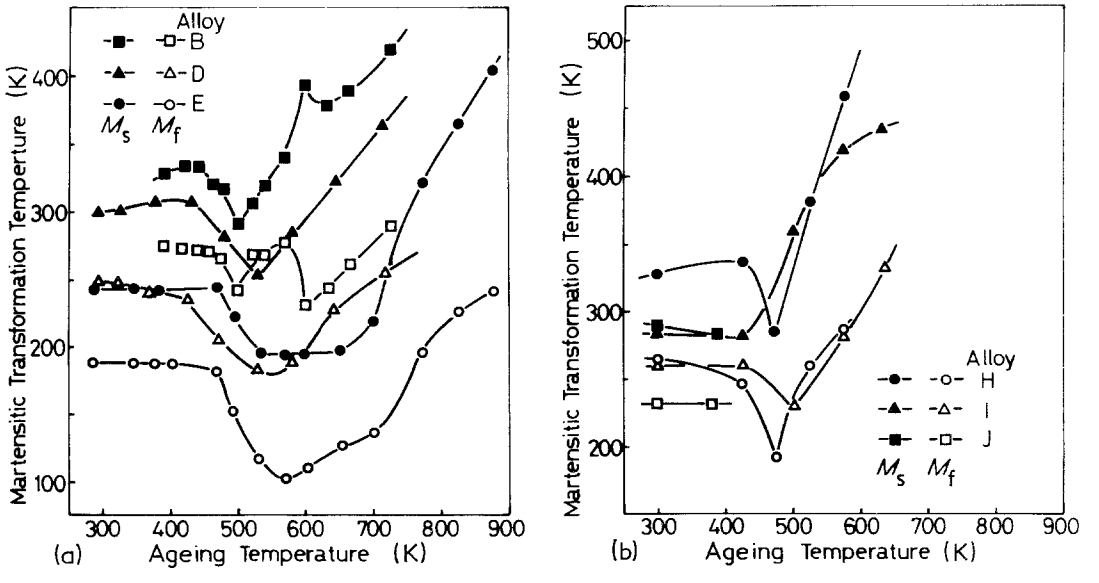

Figure 3 Effect of ageing temperature on the M_s temperature of (a) alloys B, D and E in the Cu–Al–Mn system, and (b) alloys H, I and J in the Cu–Al system.

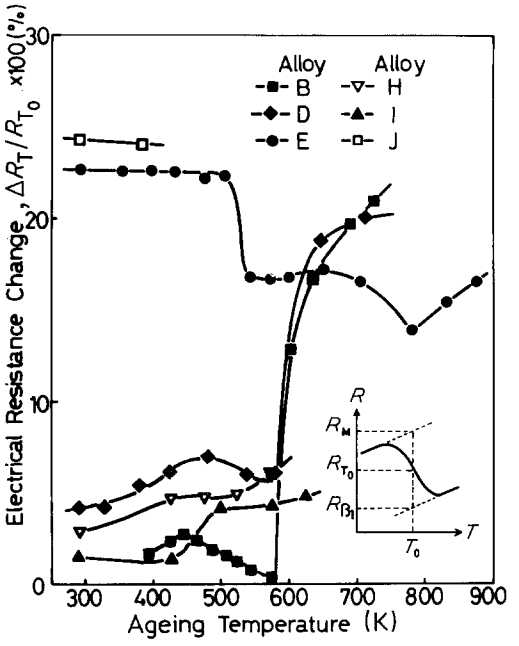

Figure 4 Effect of ageing temperature on electrical resistance change accompanied by martensitic transformation.

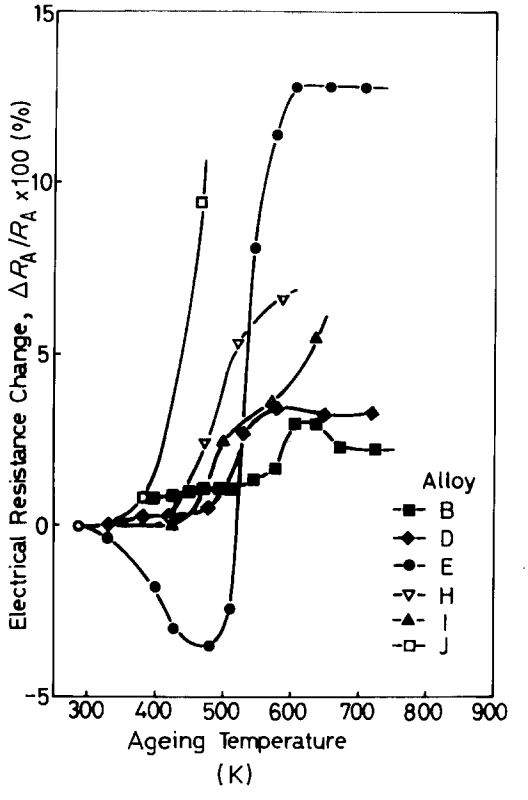

Figure 5 Effect of ageing temperature on accumulated electrical resistance change during ageing for 30 min at each temperature. R_A denotes the value of electrical resistance changing from as-quenched state and R_A means the initial electrical resistance at an ageing temperature.

alloy I after being aged at 626 K. A decrease of electrical resistance accompanied by a reverse transformation was overcome by an increase of electrical resistance due to decomposition from martensite to γ_2, as will be described later.

Electrical resistance–temperature plots of alloy J are shown in Fig. 2f. The plot profile in the as-quenched state was similar to that in the aged state at 381 K. The M_s and M_f temperatures in the as-quenched state were ~290 and ~230 K, respectively. Electrical resistance increased markedly during ageing at 466 K. After this ageing, there appeared no inflection point accompanied by a martensitic transformation on the electrical resistance–temperature curve.

3.2. A change in electrical resistance during ageing

Accumulated changes from as-quenched specimens in electrical resistance ΔR_A, occurring during the ageing of alloys B, D, E, H, I and J, are shown in Fig. 5. Electrical resistance of alloy B increased a little during ageing at temperatures below 575 K, and its increase became much larger at 600 K and was smaller above 670 K again. On the other hand, the electrical resistance of alloy E decreased considerably during ageing in the temperature range of 400 to 475 K and inversely increased largely on ageing at temperatures above 540 K. The ageing temperature at which the ΔR_A value varied from a decrease to an increase corresponded to that of which value of ΔR_T decreased the most, as seen from Fig. 4. The value of R_A for alloy D always increased slightly during ageing below 478 K and increased much above 530 K. In the alloys B, D and E, which are in order of effective aluminium content, the value of ΔR_A became smaller on ageing at temperatures lower than 500 K and larger at ones higher than 550 K.

The value of ΔR_A for alloy H became a maximum on ageing at ~500 K and decreased on ageing at higher temperatures. On the other hand, for alloy J, it increased markedly during ageing at 450 K, with this remarkable increase resulting from the precipitation of a large amount of γ_2. It was found that value of ΔR_A for Cu–Al binary alloys containing more aluminium became higher at high ageing temperatures, similar to the case of Cu–Al–Mn alloys.

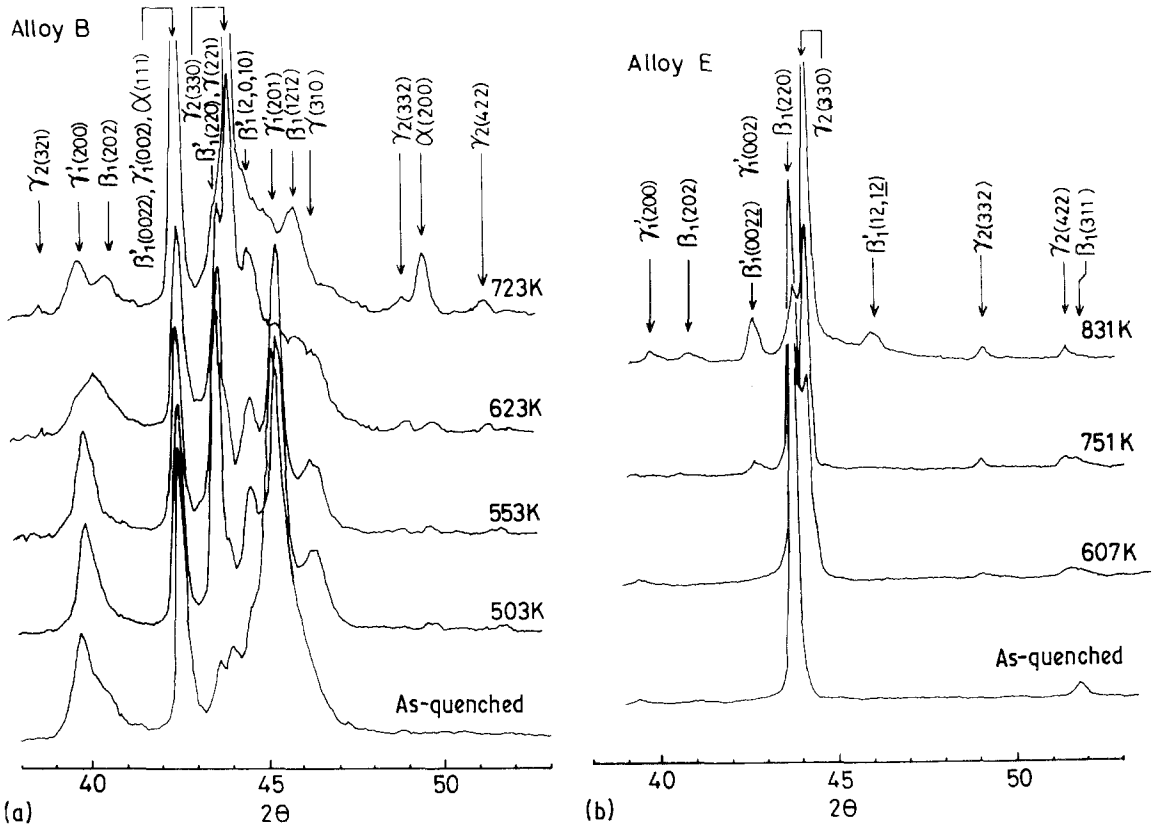

Figure 6 X-ray diffraction patterns at room temperature for alloys B, E, H and I aged at temperatures, given in figure, are shown in (a), (b), (c) and (d), respectively.

3.3. Decomposition of a β_1 phase on ageing

X-ray diffraction patterns of alloys B, E, H and I aged at various temperatures are shown in Fig. 6. Using the published data [8–12], peaks in the patterns were identified. Peak intensity of each phase present in specimens of alloys B and E was measured, and is illustrated against ageing temperature in Fig. 7.

The X-ray diffraction pattern of the as-quenched specimen of alloy B consisted of the peaks of γ_1' and β_1' martensites and γ and γ_2 as seen from Fig. 6a. The latter stable phases were little in quantity. With an elevated ageing temperature the (3 1 0) or (2 2 1) peak intensity of γ increased to a maximum at 503 K and then decreased. On the other hand, γ_2 increased markedly in quantity at ageing temperatures higher than 623 K, while α appeared at ageing temperatures above 623 K, though it was much less than γ_2, as seen from Fig. 7a. In this alloy, there existed two kinds of martensites, γ_1' and β_1'. The intensity of the (2 0 1) diffraction line of γ_1' decreased with elevating ageing temperature and became very weak on ageing at 623 K, while the peak intensity of the (1 2 12) diffraction line of β_1' became stronger at ageing temperatures higher than 623 K.

The as-quenched specimen of alloy E contained only β_1 at room temperature as seen from Fig. 6b. The (3 3 0) diffraction line of γ_2 appeared strongly on ageing at 520 K, and as the ageing temperature was increased, its peak intensity increased (see Fig. 7b). On ageing at 751 K, the peak of γ_1' martensite appeared. This means that the M_s temperature of alloy E aged above 750 K became higher than room temperature, as expected from Figs. 2c and 3a. When the specimen was aged at 831 K, the amount of γ_2 markedly increased and γ_1' and β_1' martensites also increased in quantity as a result of a considerable rise in the M_s temperature, in spite of the decomposition of β_1' to γ_2 but not α.

Alloy D was similar to alloy B in view of the electrical resistance–temperature curve in as-quenched and aged sample and their composition. Therefore, the decomposition behaviour of alloy B may be basically similar to alloy D.

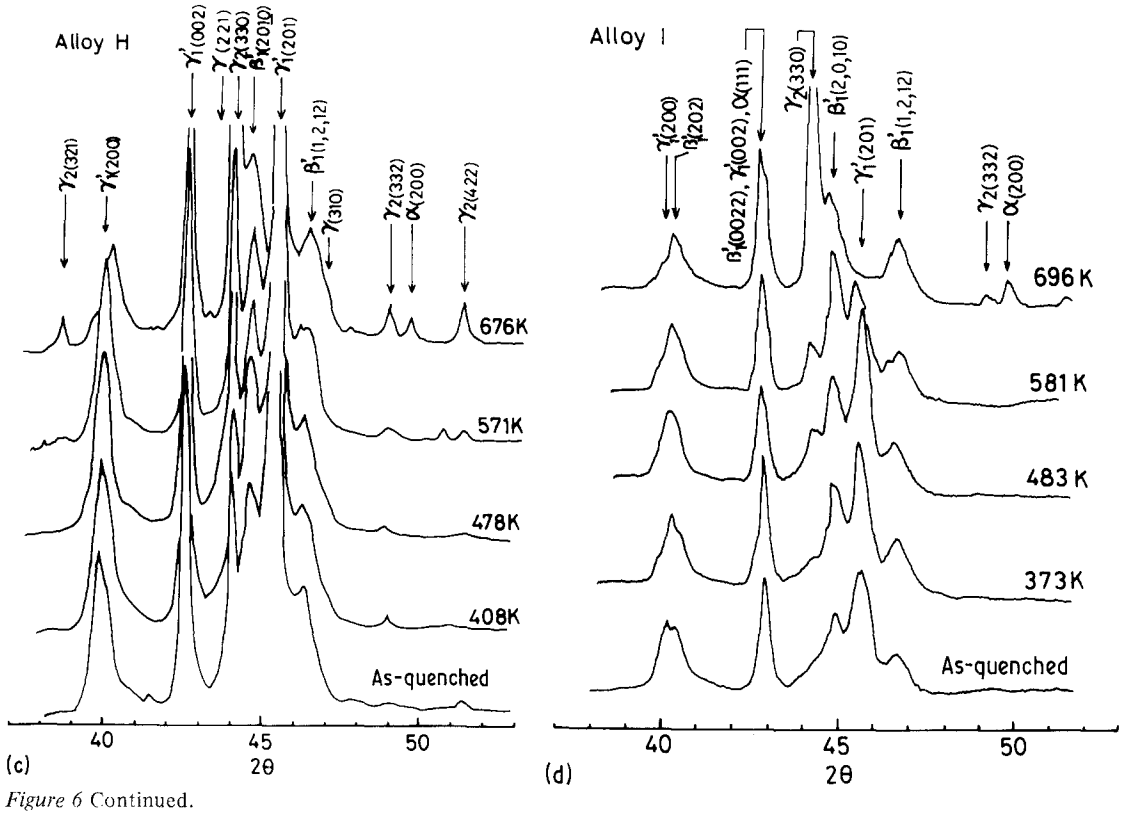

Figure 6 Continued.

The as-quenched specimen of alloy H contained β_1' and γ_1' martensites and γ_2 as seen from Fig. 6c. As expected from the phase diagram, the quantity of γ_1' was much more than that of β_1'. The amount of γ_2 which precipitated in the as-quenched state increased with rising ageing temperature. The (310) and (221) diffraction lines of γ could be detected slightly on ageing at 478 K and α was found on ageing at 676 K.

The as-quenched specimen of alloy I contained β_1' and γ_1' martensites, as seen from Fig. 6d. The (330) diffraction line of γ_2 appeared on ageing at

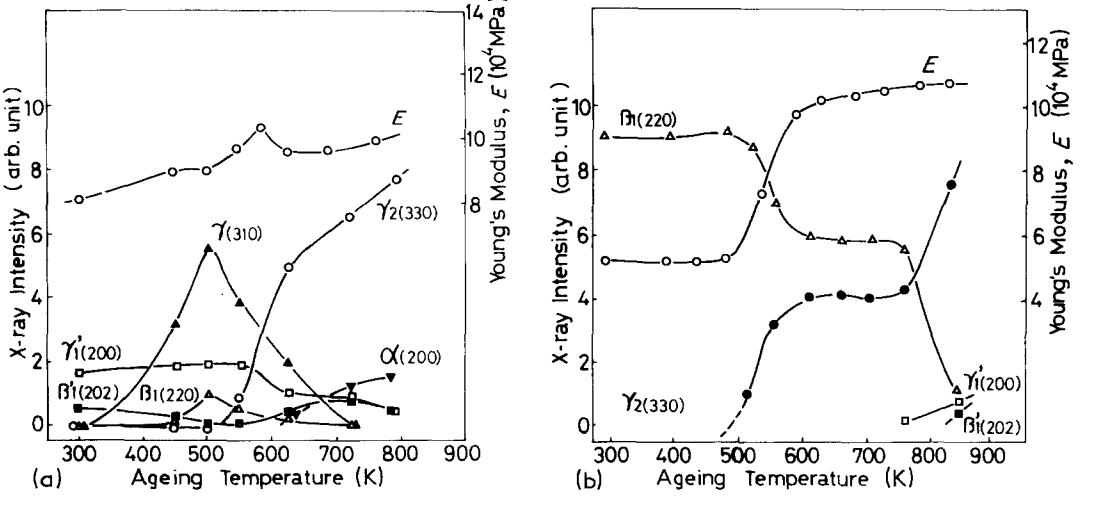

Figure 7 Effects of ageing temperature on Young's modulus and the peak intensity of X-ray diffraction lines for alloys B, and E, are shown in (a) and (b), respectively. The X-ray intensity was given from the peak height of each diffraction line.

483 K and its peak intensity gradually increased with rising ageing temperature. On ageing at 696 K, the (200) diffraction line of α appeared and the specimen reversely transformed no longer from martensite (see Fig. 2e). The (201) diffraction intensity of γ_1' martensite decreased with raising ageing temperature, on the contrary, the (1 2 12) diffraction intensity of β_1' martensite increased with rising ageing temperature.

4. Discussion

4.1. Effect of manganese on the M_s temperature in the as-quenched state

It is well known that the M_s temperature of as-quenched copper–aluminium binary alloys is largely dependent on the aluminium concentration in the β_1 phase. The M_s temperature of the as-quenched specimens measured in the present work was plotted against the effective aluminium content, [%Al/(%Cu + %Al)] x 100, in Fig. 8. Although some specimens contained stable phases in the as-quenched state, the effective aluminium concentration of the β_1 phase in their as-quenched specimens should be approximate to the effective aluminium content of the specimens because of only a small amount of stable phases in the β_1 phase. A solid line through open square points represents the relationship between the M_s temperature and effective aluminium concentration of β_1 for Cu–Al binary alloys. The M_s temperature of Cu–Al–Mn alloys became lower than that of Cu–Al binary alloys with the same effective aluminium content as the former and an increase in manganese content lowered the M_s temperature. From Fig. 8, it is concluded that 1 wt % manganese has an effect to cause the M_s temperature in the as-quenched state to lower by about 30 K.

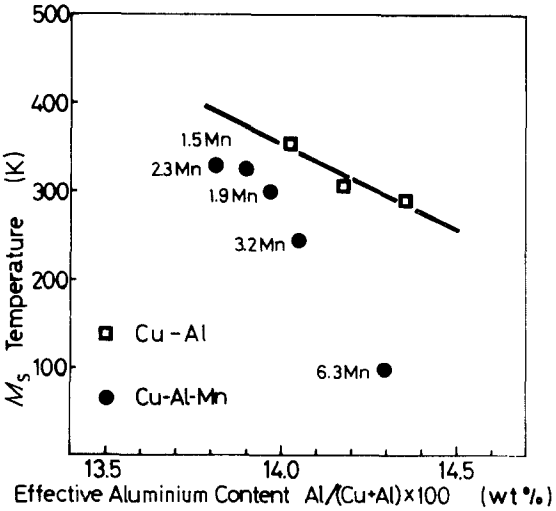

Figure 8 The relation between the effective aluminium concentration and M_s temperature in the as-quenched state.

4.2. Ageing effect on the M_s temperature

As mentioned above, the M_s temperature of Cu–Al–Mn alloys in the as-quenched state depended on the effective aluminium concentration and manganese concentration in the β_1 phase. The lowest M_s temperature in the alloy B series was obtained on ageing at 500 K, corresponding to the highest aluminium concentration in β_1, because the greatest quantity of γ (an aluminium-poor phase) precipitated at 500 K, as seen from Figs. 6b and 7a. On ageing at a higher temperature above 500 K, the M_s temperature of alloy B rose, which can be explained by the reason of a decrease and an increase in the quantity of γ_2 and hence a lowered aluminium concentration in β_1. When the ageing temperature rose to 630 K, γ_2 precipitated and thus the aluminium concentration in β_1 must have increased, which lowered the M_s temperature again. The relationship between M_s temperature and ageing temperature for alloy B is qualitatively based on the aluminium concentration resulting from the instability of the β_1 phase at the ageing temperature. The M_s temperature of alloy H became a minimum on ageing at 475 K, which would be due to the precipitation of γ on ageing, as seen from Fig. 6c. An increase of the M_s temperature with a rise in ageing temperature above 475 K might result from precipitating a greater quantity of γ_2 at the higher temperature.

The aluminium concentration in β_1 of alloy I decreased with rising ageing temperature as a result of the precipitation of an aluminium-rich phase, i.e. γ_2. Therefore, the M_s temperature rose on ageing at a higher temperature above 480 K. The M_s temperature of alloy I had no minimum since γ hardly precipitated.

On ageing at temperatures up to 483 K no precipitates were observed in specimens of alloy E and the M_s temperature also unchanged. With a rise in the ageing temperature from 483 to 600 K, γ was hardly precipitated, while the quantity of γ_2 increased. Nevertheless, the M_s temperature was lowered by 50 K. This change in the M_s temperature was not compatible with a variation in the aluminium concentration in β_1. Values of electrical resistance changing during ageing within this

ageing temperature range increased remarkably from −4% to 12%, as shown in Fig. 5. It has been found that thermoelastic martensitic transformation occurs easier in materials with a smaller shear modulus and larger elastic anisotropy [13–15]. Shear modulus G is expressed as follows;

$$G = E/(2 + 2\nu)$$

where E is Young's modulus and ν is Poisson's ratio. Therefore, if Young's modulus in β_1 were known, decreasing the M_s temperature was explained by a Young's modulus change. Young's modulus was measured by the flexural vibration method. The resonant frequency, f_0, of the specimens, whose size was 2 mm × 10 mm × 100 mm, for Young's modulus measurements were about 800 Hz and the strain amplitude was 8×10^{-6}. Young's modulus, E, was calculated as follows;

$$E = 946.8 \frac{l^3 g}{t^3 w} f_0^2$$

where l, t, w and g are the length, thickness, width and weight of a specimen, respectively, in SI units.

Young's modulus of aged specimens of alloys B and E was measured at room temperature. In the case of alloy E, Young's modulus of specimens aged above 600 K became twice as large as that of specimens aged below 483 K. It is known from Fig. 7 that such a change in Young's modulus is considerably large as compared with the case for alloy B. Having Young's modulus increased by a factor of two times will result in the shear modulus increasing two times. An increase in Young's modulus, therefore, must make the martensitic transformation of β_1 difficult and thus the M_s temperature low, though precipitation of γ_2 can elevate the M_s temperature. Precipitation of a large amount of γ_2 from β_1 on ageing above 750 K would be the reason why the M_s temperature rose at these temperatures.

4.4. Effects of the degree of ordering and vacancy concentration in the supercooled β phase on the M_s temperature

With a rise in the ageing temperature of alloy E to 400 K, no precipitates were formed, while the electrical resistance decreased (see Fig. 5). This means that either the degree of ordering in the supercooled β phase increased or quenched-in vacancies annealed out. On the other hand, the M_s temperature was unchanged on ageing within this temperature range. Therefore, it may be concluded that the degree of ordering or the vacancy concentration had no effect on the M_s temperature.

4.5. Effect of ageing on the martensitic transformation temperature range and the transformation hysteresis

A martensitic transformation temperature range, M_s–M_f, would also relate to the easiness of martensitic transformation. It extended largely at ageing temperatures at which a large amount of γ_2 precipitated in all experimented alloys. It is evident from Figs. 5, 7 and 9 that precipitates of γ_2 caused not only enlargement of the transformation temperature range but also an increase of the ΔR_A value. These agree with the results of Kennon *et al.* [16] who found that precipitates of γ_2 obstructed the growth of martensite plates. On the other hand, a large amount of γ precipitated in alloy B on ageing at 500 K, but it could have an effect on the transformation temperature range. Decreases of the transformation temperature range of alloys B and I on ageing at 700 and 620 K, respectively, may result from a decrease in retained β_1 in quantity due to precipitation of stable phases.

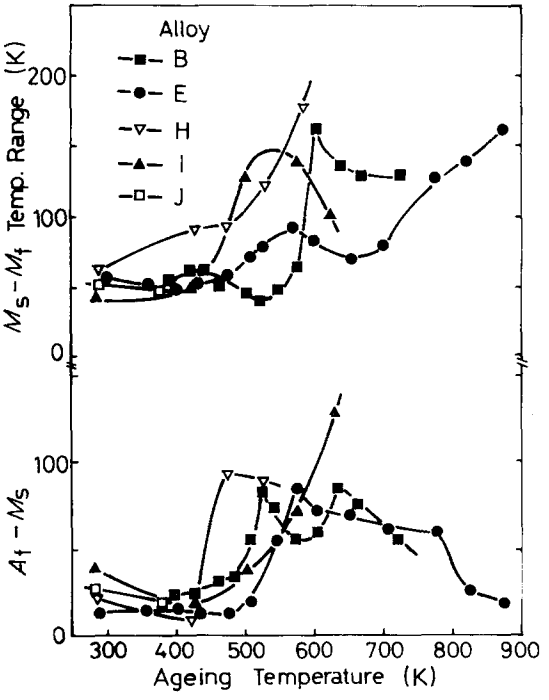

Figure 9 Influence of ageing on the martensitic transformation range given by M_s–M_f and the transformation hysteresis given by A_f–M_s.

Transformation hysteresis which is represented by the temperature range between A_f and M_s temperatures is shown as a function of ageing temperature in Fig. 9. It relates to the ease of nucleating martensite or austenite. Alloys B, D, E, H, I and J increased hysteresis above the ageing temperature of about 500 K. At this temperature, a lot of precipitates of γ or γ_2 appeared in the matrix. The nucleation of martensite might be deterred because γ or γ_2 precipitated favourably at nucleation sites in the matrix. Comparing the hysteresis of alloys E and H which are of approximately same effective aluminium content, it is found that manganese prevents the hysteresis from increasing.

4.6. Effect of composition on stability of β_1

Fig. 10 shows the relation between the temperature at which β_1 decomposes entirely and the effective aluminium concentration for all the alloys. The decomposition temperature of β in Cu–Al binary alloys decreased with increasing aluminium content because γ_2 could precipitate more easily in β_1 as this phase was of higher aluminium concentration. The decomposition temperature of β_1 in Cu–Al–Mn alloys increased with increasing manganese content. The addition of 1 wt% manganese into Cu–Al binary alloys increased the decomposition temperature by about 80 K. Manganese is, therefore, a useful stabilizing element for β_1. This is one of the necessary conditions for utilizing Cu–Al–Mn alloys industrially.

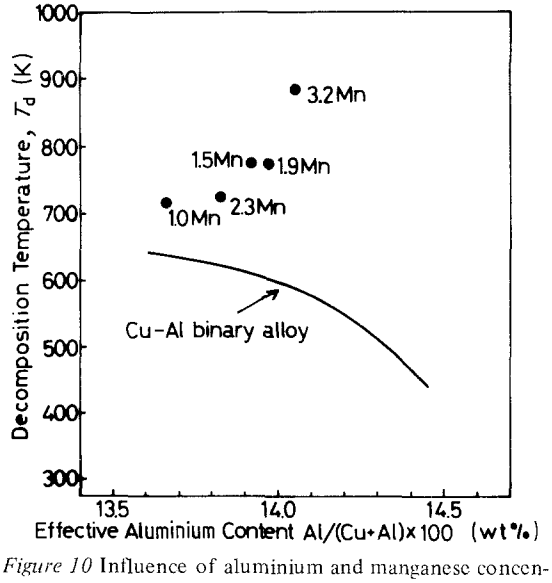

Figure 10 Influence of aluminium and manganese concentration on decomposition temperature of Cu–Al and Cu–Al–Mn alloys.

5. Conclusion

The influences of ageing and manganese on the M_s temperature of Cu–Al–Mn alloys were examined by electrical resistance and X-ray diffraction methods. The M_s temperatures of many aged alloys were closely related to the aluminium concentration in β_1 which changed as a result of precipitating α, γ and γ_2 phases. In the case of a few alloys, the elastic modulus of β_1 was a factor influencing the M_s temperature.

Manganese made the M_s temperature lower by about 30 K per 1 wt% addition.

The addition of manganese into Cu–Al alloys could also restrain the precipitation of the stable phase from β_1.

The martensitic transformation temperature range and transformation hysteresis of Al–Cu–Mn alloys were made larger by the precipitation of γ_2 and α and γ, respectively. Since manganese had an effect to suppress the precipitation of γ_2, unvaried transformation hysteresis for alloys containing manganese did not vary on ageing at high temperatures.

References

1. K. SUGIMOTO, T. MORI, K. OTSUKA and K. SHIMIZU, *Scripta Metall.* 8 (1974) 1341.
2. W. DEJUNGE, L. DELAEY, R. DEBATIST and J. VAN HUMBEECK, *Met. Sci.* 10 (1977) 523.
3. K. OTSUKA, *Jpn. Appl. Phys.* 10 (1971) 571.
4. L. G. KHANDROS, *Phys. Met. Metall.* 48 (1979) 110.
5. F. NAKAMURA, J. KUSUNOI, Y. SHIMIZU and J. TAKAMURA, *Nippon Kinzoku Gakkaishi* 44 (1980) 1302.
6. T. SUZUKI, M. TAKAGI, A. NAGASAWA and N. NAKANISHI, *J. Mater. Sci.* 16 (1981) 3013.
7. R. G. COPE, *J. Inst. Met.* 87 (1958) 330.
8. P. P. JEWETT and D. J. MACK, *J. Inst. Met.* 92 (1963–64) 59.
9. S. K. SESHADRI and D. B. DOWIN, *Met. Sci.* 13 (1979) 696.
10. H. WARLIMONT and M. WILKENS, *Z. Metallkd.* 55 (1964) 382.
11. W. GAUDIG and H. WARLIMONT, *ibid.* 60 (1969) 488.
12. J. S. LLEWELYN LEACH, *J. Inst. Met.* 92 (1963) 93.
13. Y. JEFEN, J. MAKOVSKY and M. ROSEN, *J. Phys. Chem. Solid.* 38 (1977) 647.
14. A. PRASETYO, F. RAYNAUD and H. WARLIMONT, *Acta Metall.* 24 (1976) 651.
15. O. MERCIER, K. N. MELTON, G. GREMAUD and J. HAGI, *J. Appl. Phys.* 51 (1980) 1833.
16. N. F. KENNON, D. P. DUNE and L. MIDDLETON, *Metall. Trans. A.* 13A (1982) 551.

Received 22 November 1983
and accepted 30 April 1984